Electronic Supplementary Material (ESI) for Journal of Materials Chemistry C.

Supporting Information for

Strain to Alter the Covalency and Superconductivity in Transition Metal Diborides

Huanchen Zhai,[1] Francisco Munoz,[2,3,*] Anastassia N. Alexandrova[1,4,*]

[1]*Department of Chemistry and Biochemistry, University of California, Los Angeles, Los Angeles, CA, 90095, USA*

[2]*Departamento de Física, Facultad de Ciencias, Universidad de Chile, Chile*

[3]*Center for the Development of Nanoscience and Nanotechnology CEDENNA, Santiago, Chile*

[4]*California NanoSystems Institute, Los Angeles, CA, 90095, USA*

Corresponding Authors e-mails: fvmunoz@gmail.com, ana@chem.ucla.edu

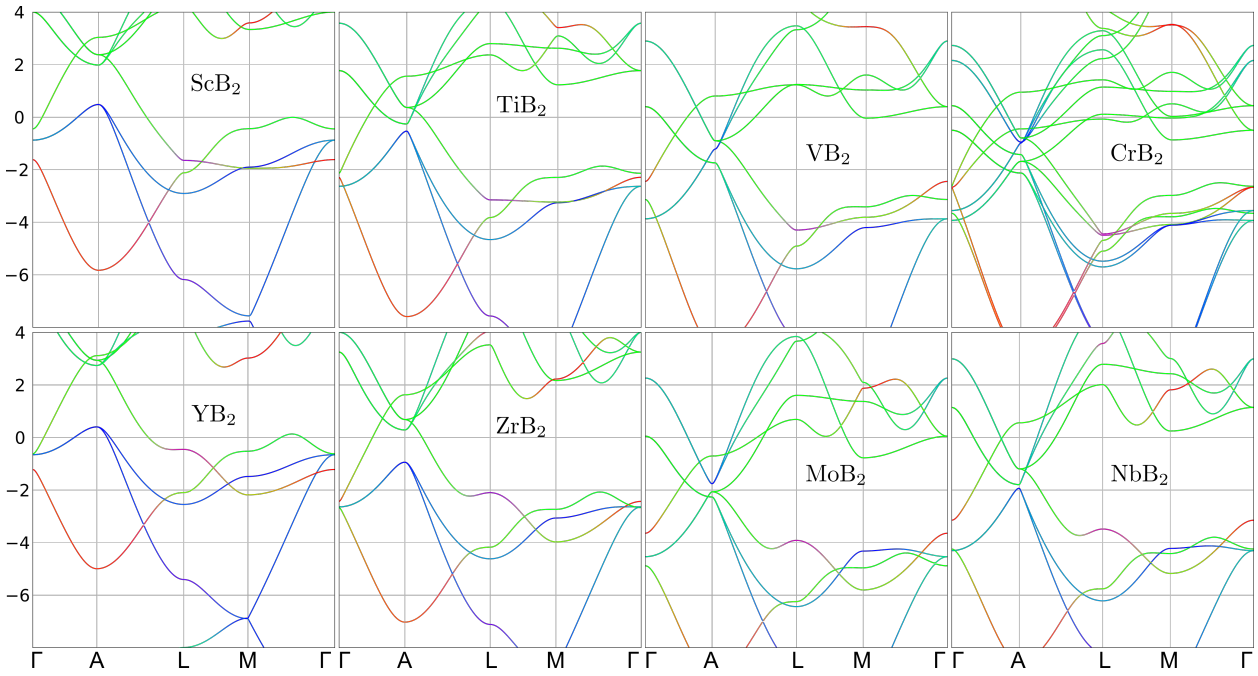

Figure S1. Band structures of the MB_2 materials. The bands are tinted in red according to their projection on the sp_2 orbitals of the B atoms. CrB_2 is spin-split.

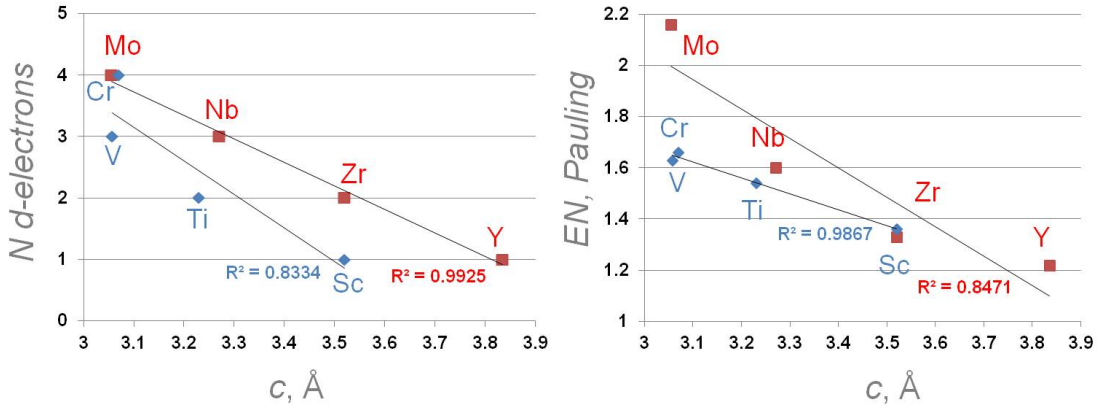

Figure S2. Correlations between the lattice *c* parameter and (left) the number of d-electrons in the metal, and (right) the Pauling electronegativity.

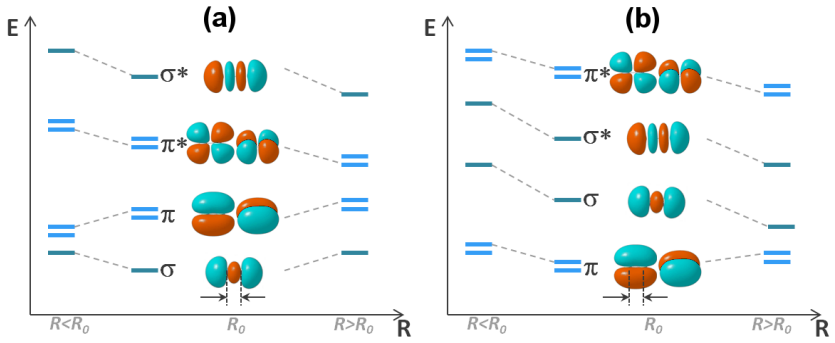

Figure S3. Schematics of the trends of the energies of the σ- and π-MOs in diatomics upon compression and elongation along the bond: (a) the regular case where the σ-bond is more stable than the π-bond, characteristic of larger diatomics, such as C_2; (b) the regular case where the π-bond is more stable than the σ-bond, characteristic of larger diatomics, such as B_2.

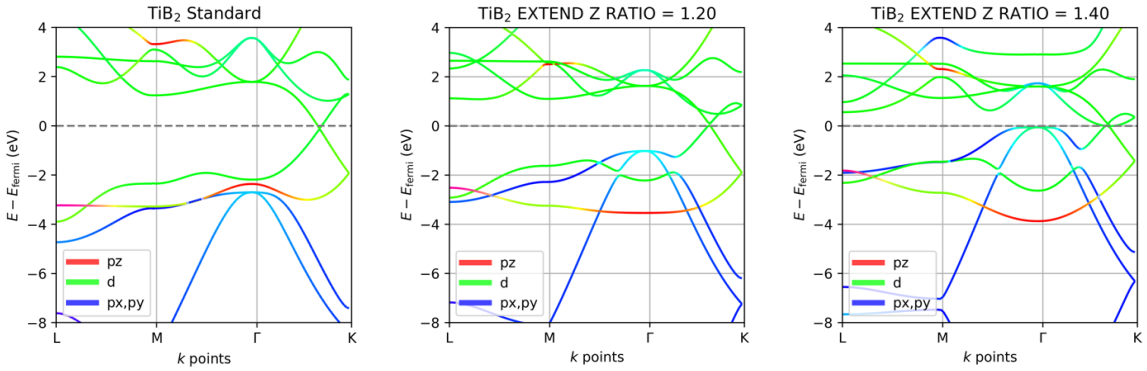

Figure S4. The band structures of TiB_2 with cell parameters along *z* direction being 100%, 120%, and 140% (from left to right) of the optimized cell parameters (*c* = 3.2232 Angstrom).

	atom Sc	atom B_1	atom B_2
100% *c* parameter	+1.48	-0.80	-0.67
120% *c* parameter	+1.40	-0.76	-0.63

Table 1. The Bader charges of each atom in ScB_2 in optimized structure and the structure with *c* parameter being 120% of the optimized value.

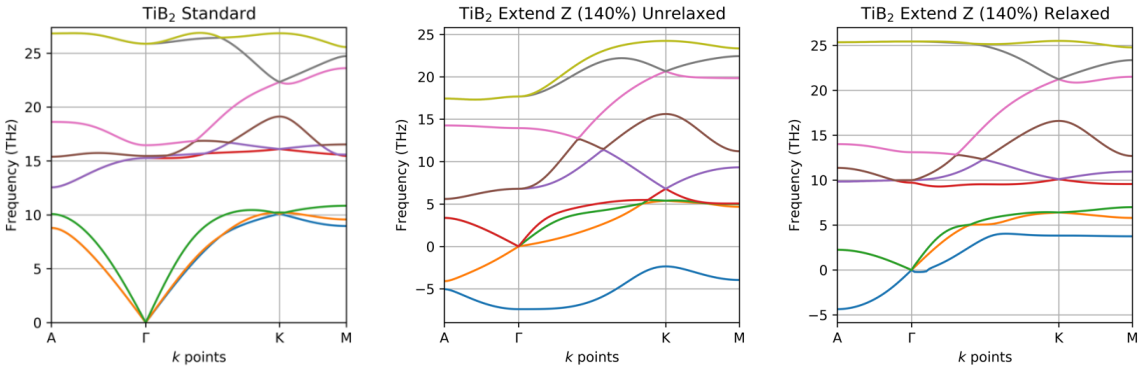

Figure S5. Phonon spectra of TiB_2 of optimized structure and the structure with *c* parameter being 140% of the optimized value. For the increased *c* case, the phonon spectra for the structure with atomic position unchanged and relaxed are plotted separately. The yellow band from A to Gamma *k*-points is the E_{2g} band.

From Figure S4 we can see that to push p-σ band up to Fermi level, we need to extend *c* parameter by 40%. However, this will also introduce imaginary frequency at the Gamma point (Figure S5), and that suggests that under a large strain the system would become unstable. If we optimized the structure with increased *c* parameter, another imaginary frequency at the A point appears. From this we can see that there is a spontaneously symmetry breaking to happen under stress along the *z* direction. The energy will become lower if we decrease the symmetry along *z* axis. However, clearly this will change the structure from the original.

The studies on ZrB_2 and HfB_2 are presented blow in Figures S6-S8, for completeness. From the band plot we can see that, similar to the TiB_2 case, the π-sigma band is far away from the Fermi level. In addition, the phonon band shows that E_{2g} phonon is not coupled with the electronic π-σ band, in HfB_2. ZrB_2 shows very similar behavior. Therefore, changing the cell size is unlikely to induce the superconductivity in these two systems.

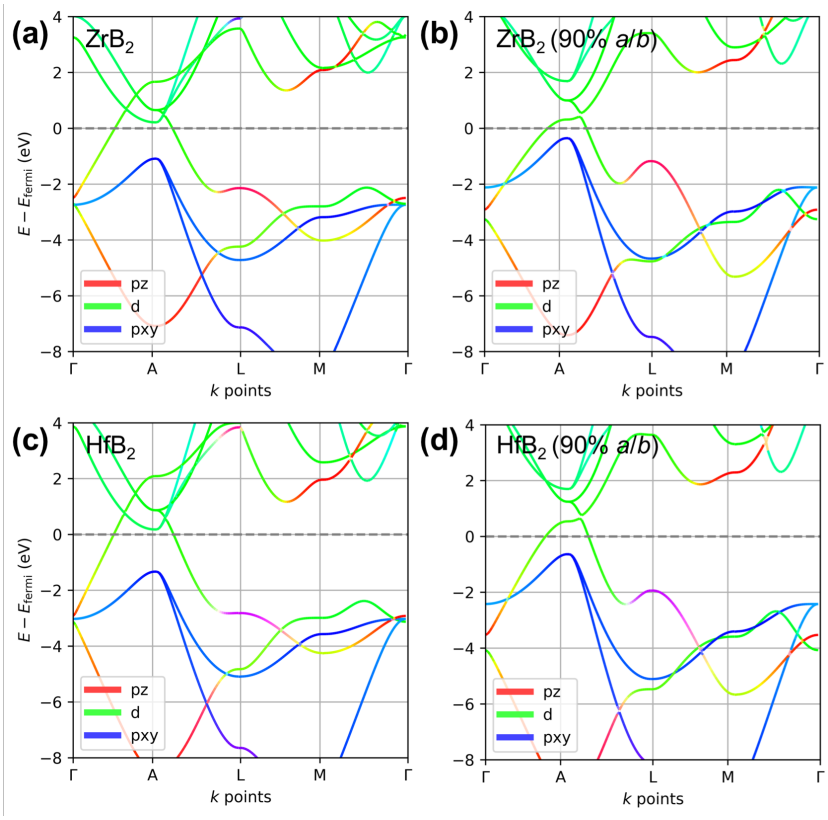

Figure S6. The band structures of (a-b) ZrB_2 and (c-d) HfB_2 with cell parameters along *a* and *b* direction being 100% and 90% (from left to right). The optimized cell parameters *a* for ZrB_2 and HfB_2 are 3.1725 and 3.0351 Å, respectively.

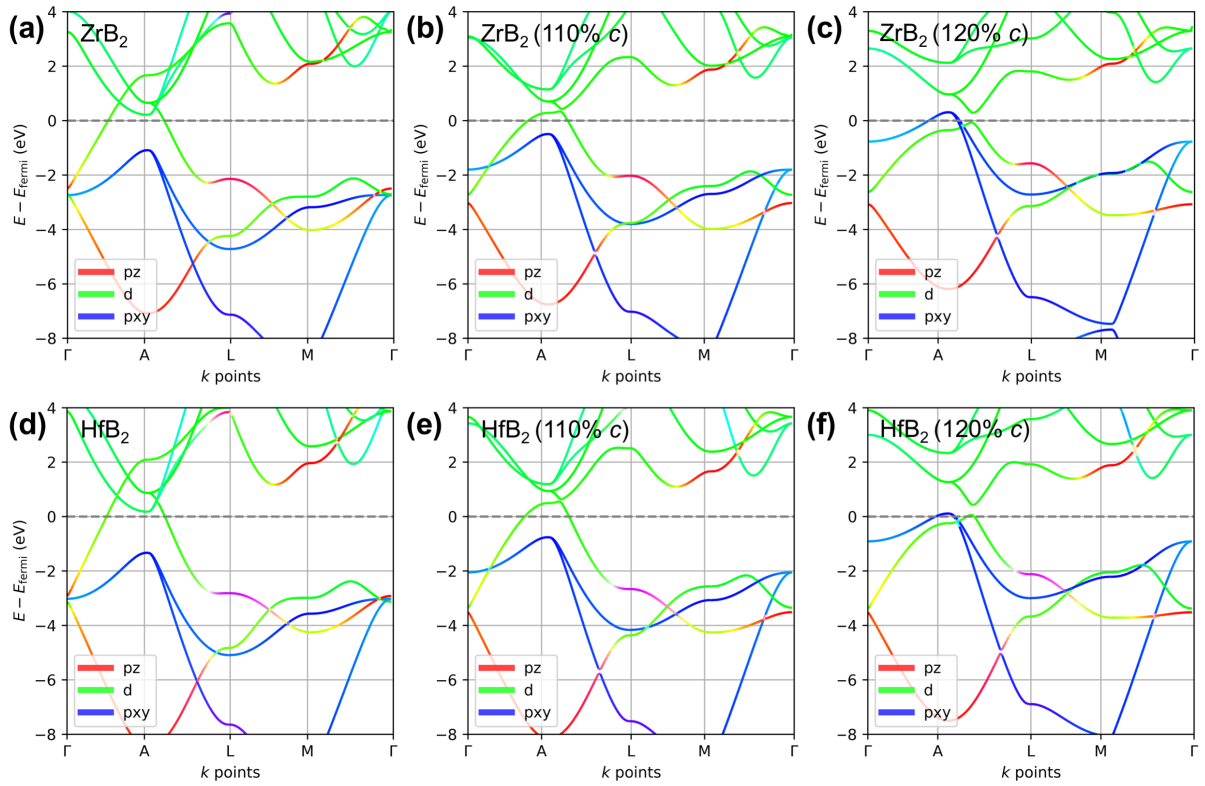

Figure S7. The band structures of (a-c) ZrB_2 and (d-f) HfB_2 with cell parameters along *c* direction being 100%, 110%, and 120% (from left to right). The optimized cell parameters *c* for ZrB_2 and HfB_2 are 3.5419 and 3.4844 Å, respectively.

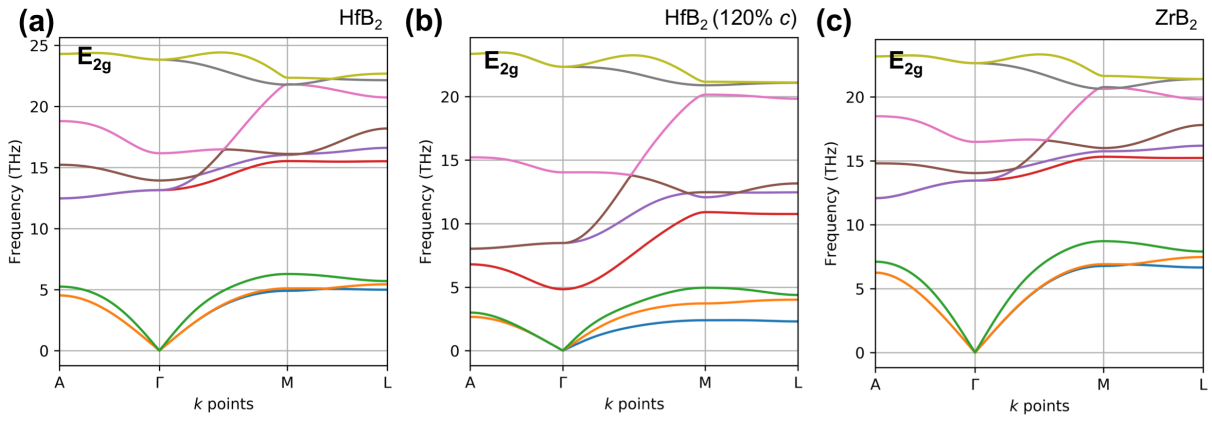

Figure S8. Phonon spectra of (a) HfB_2 and (c) ZrB_2 at equilibrium, and (b) HfB_2 upon applied elongation along c.

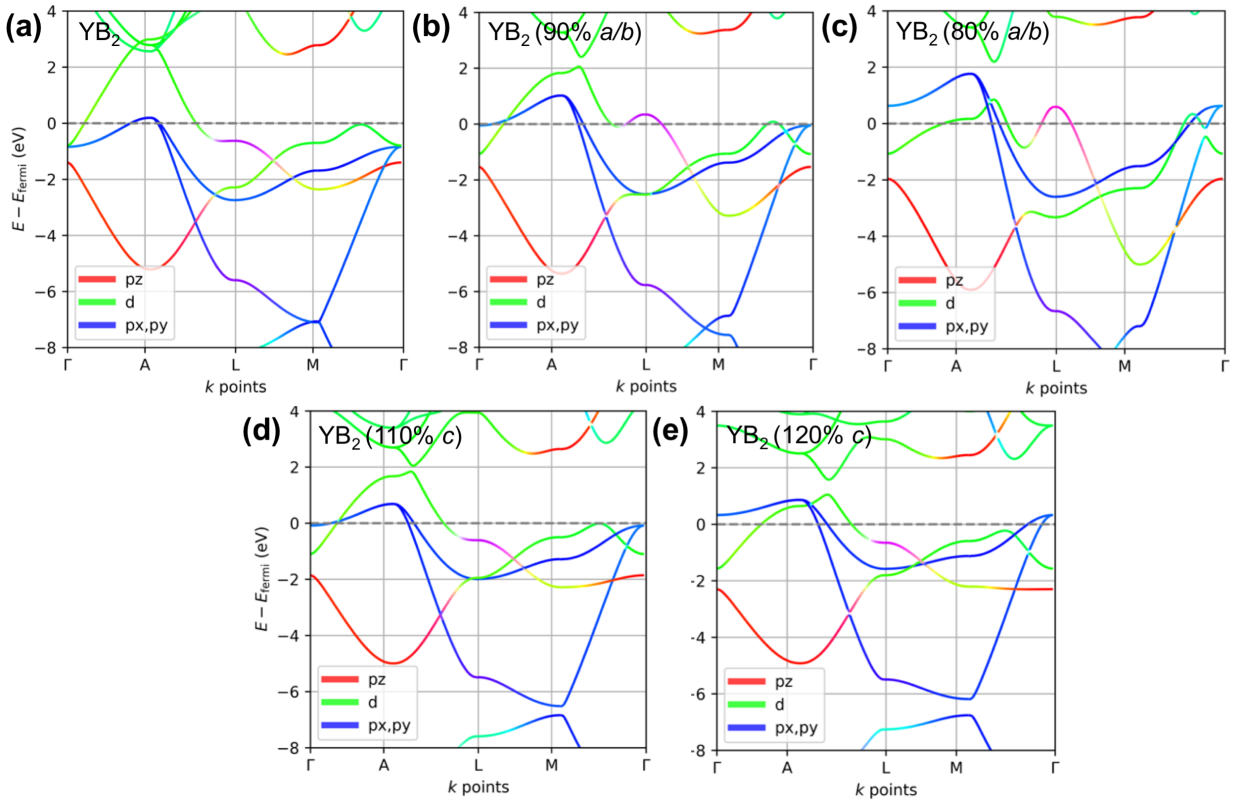

Figure S9. The band structures of (a) YB_2 and with cell parameters (b-c) along *a/b* direction being 90% and 80% and (d-e) along *c* direction being 110% and 120%. The optimized cell parameters a/b and *c* for YB_2 are 3.002 and 3.863 Å, respectively.

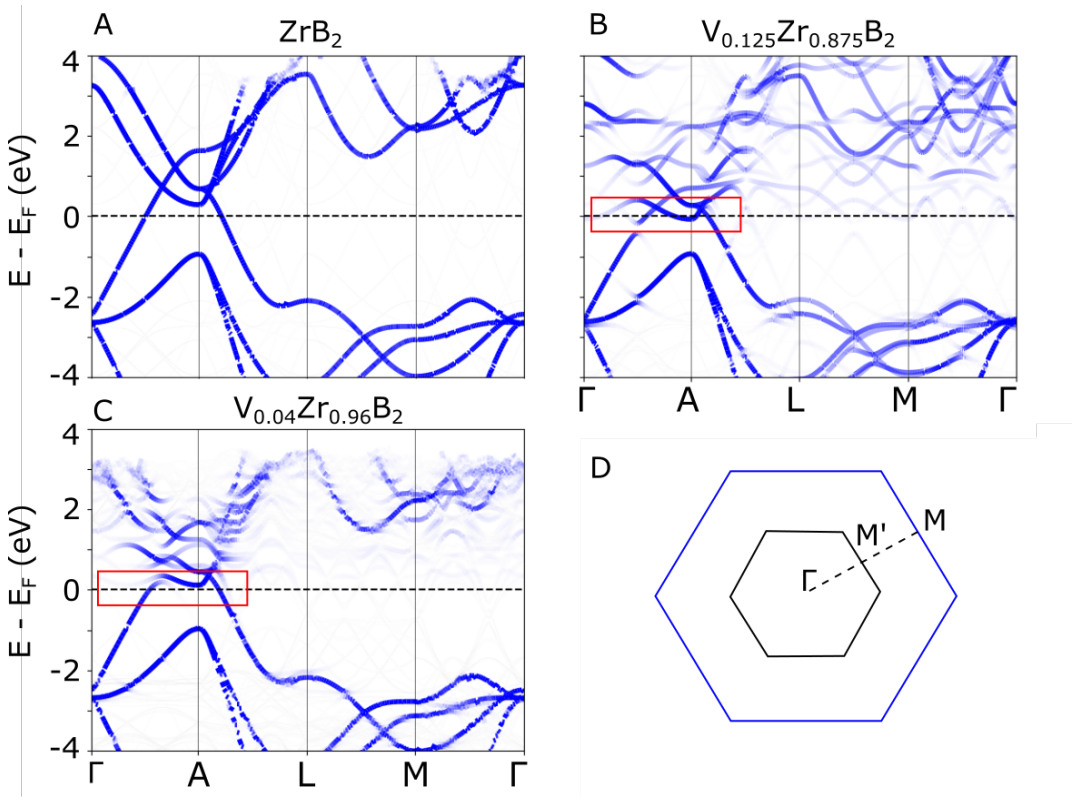

Figure S10. Unfolded band structure of a ZrB2 supercell with a V substitutional impurity. The supercell are (B) 2x2x2, with a stoichiometry $V_{0.125}Zr_{0.875}B_2$ and (C) 3x3x3 with stoichiometry $V_{0.04}Zr_{0.96}B_2$. Panel (A) shows the bands of pristine ZrB2 for the sake of comparison. Panel (D) shows the Brillouin zone of the 2x2x2 supercell (black) inside the Brillouin zone of the primitive lattice. The unfolding procedure projects the wavefunctions of the supercell on the primitive lattice.

Figure S10 shows the unfolded band structure of V-doped ZrB_2. That is the projection of the supercell Brillouin zone back on the primitive Brillouin zone. Since the wavefunctions are not eigenfunctions of the primitive Brillouin zone, their projection on it has a linewidth, represented by the color intensity of the bands. A more detailed explanation can be found in P. B. Allen et al. Phys Rev B 87, 085322 (2013).

An small addition of V has several effects, that combined can give a plausible explanation of the emergence of superconductivity. In the figure S10B,C it is evident that the Fermi level moves very close to the bottom of the dxz, dyz band (surrounded by a red box). Also that band adopts a flat-like shape along the Γ-A line. In addition, these bands are degenerated, by symmetry. All these factors suggest a large rearrangement of the Fermi surface due to a suitable phonon. Such a phonon mode should break the dxz-dyz degeneracy, just in the same way the E_{2g} mode breaks the degeneracy of the σ band.